Effect of Fluid Flow on Pressure Drop in a Porous Medium of a Packed Bed

A.A. Adeyanju
Department of Mechanical and Manufacturing Engineering,
University of West Indies, St. Augustine, Trinidad and Tobago, Nigeria

Abstract: The velocity variation within the porous medium depends on the structure of the packed bed. This behaviour exhibits hydrodynamic mixing at the pore scale. The pressure drops occurring across the porous medium is attributed to several factors, including form drag, viscous drag from bounding wall and inertia force. The obtained results from this study confirm that the pressure drop is a linear function of flow velocity at low Reynolds number regime and a quadratic function at higher Reynolds numbers. The morphological effect is an additional factor in determining pressure drop.

Key words: Porous medium, packed bed, pressure drop, Reynolds number, velocity, linear function

INTRODUCTION

Natural and manufactured porous materials have broad applications in engineering processes, including flow straighteners, heat sinks, mechanical energy absorbers, catalytic reactors, heat exchangers, pneumatic silencer, high breaking capacity fuses and cores of nuclear reactors. For the subject of flow, pressure drop and heat transfer through porous media, there have been extensive investigations covering broad ranges of applications since, the early research of Darcy in the 19th century. Darcy correlated the pressure drop and flow velocity experimentally by defining a special constant property of the medium called permeability. However, it is only applicable to low speed (creeping) flow and low porosity saturated medium. It is well known that in flow through porous media the pressure drop caused by the frictional drag is proportional to the velocity at the low Reynolds number range. In addition, this famous Darcy's law also neglects the effects of solid boundary and the inertial forces on fluid flow and heat transfer.

Fluid transport is usually modeled using the continuum approach in terms of appropriate averaged parameters in which the real pore structure and the associated length scales are neglected. Moreover, those averaged parameters can only be obtained by experiments and are strongly influenced by the types of microstructure and operating conditions. Fundamentally, they are limited to the scope of macroscopic phenomena. Specifically, the microscopic (pore scale) dispersion effect has significant impacts on the mass, momentum and thermal transports. Hence, modeling transport behavior at the pore-scale for real engineering processes is desirable.

Mass and thermal transport in porous media, such as ceramics, rocks, soils and catalytic channels in fuel cells, play an important role in many engineering and geological processes. There are two interesting aspects that arise in the research of porous media. They are hydrodynamic and thermal effects. The dynamics of fluids flow through a porous medium is a relatively old topic. Since, the 19th century, Darcy's law has traditionally been used to obtain quantitative information on flow in porous medium. This law is reliable when the representative Reynolds number is low whereas the viscous and pressure forces are dominant. As the Reynolds number increases, deviation from Darcy's law grows due to the contribution of inertial terms to the momentum balance (Bear, 1972; Kaviany, 1991). It is shown that for all investigated media, the axial pressure drop is represented by the sum of two terms, one being linear in the velocity (viscous contribution) and the other being quadratic in velocity (inertial contributions). The inertial contribution is known as Forchheimer's modification of the Darcy's law (Reynolds, 1900). Basically, the pressure drop occurring in a porous medium is composed of two terms. Later Beavers and Sparrow (1969) proposed a similar model for fibrous porous media. A general expression can be obtained from Bear (1972) and is widely accepted in the Eq. 1:

$$dp/dx = - \mu u/\kappa \qquad (1)$$

It is shown that the pressure drop is directly proportional to the fluid viscosity μ and inversely proportional to the permeability of the porous medium. Large et al. (1997) suggested that an additional cubic term of fluid velocity be included in the above Eq. 1 in the regime of higher speed ($R_{\text{eox}} \approx O$ (10)). Another significant research for predicting momentum transport in porous media is by Brinkman (1947). Brinkman (1947) first introduced a term, which superimposed the bulk and

boundary effects together for flows with bounding walls. In Brinkman's model, an effective viscosity was postulated from experiments performed on beds of spheres to replace the viscosity of fluid by taking into account of the porosity effect, where, ε is the porosity.

$$\mu_{eff} = \mu \left(1 + 2.5 \left(1-\varepsilon\right)\right) \qquad (2)$$

There have been modifications on the Eq. 2 to describe different types of porous media (Sahraoui and Kaviany, 1993). More recently, computational modeling has been used to provide detailed flow fields. There are also results obtained by the asymptotic solutions (Chapman and Higdon, 1992). In this study, velocity variation in relation to pressure drop is examined.

MATERIALS AND METHODS

Numerical experiments of 2D porous flow: The schematic of the configuration is shown in Fig. 1. The direction of air flow is from left to right and the porous sample is located in the middle of the domain (20×10 cm) to allow for a well-developed flow before it reaches the porous sample and in order to minimize any numerical instability. The distance from inlet to the front side of the porous medium, is 9 cm, which is also about the range estimated by Kaviany (1991). Five representative axial positions, Δ_1-Δ_5, as shown in Fig. 1 are selected for evaluating data and interrogation of flow field; they are located, respectively upstream, starting plane, mid-plane, exit plane and downstream of the porous medium. The porous sample length is 2 cm. The flow rate varies by changing the inflow velocity u_{in}. The pressure drops are calculated based on the pressure difference across the porous sample.

Several representative pore structures have been studied. Table 1 shows structures of different porosities with two types of geometric shapes.
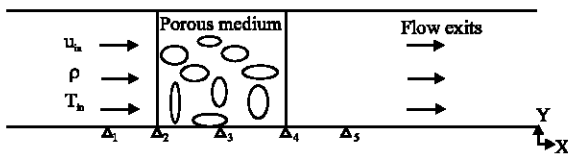

Fig. 1: Schematic of porous flow in a 2D channel and stations for flow analysis

Table 1: Morphological characteristics of porous samples used in the pressure drop study

Shape	Case	Porosity	d (mm)	No. solid elements	Total No. elements
Sphere-like	Structure 1	0.854	3	650	47,000
	Structure 2	0.890	3	454	47,000
	Structure 3	0.947	3	235	47,000
Fibrous	Case 4	0.830	0.75	1705	50,000

In the case of sphere-like porous medium, r is the radius of the sphere, while t is the thickness of fiber for fibrous solid phases. The fibrous structure is composed of slender and long fiber in sheets, in which the form drag is much small than the circular cylinder tubes structure. The total number of elements (both fluid and solid) in Table 1 is the number of total cells used in the computation.

RESULTS AND DISCUSSION

The numerical procedures are set to mimic the experiments, conducted either in wind tunnel or water tunnel. Porous samples are inserted inside a channel in two-dimension and a duct in three-dimension to simulate the experiments performed in the manner described by Hunt and Tien (1988a, b), Calmidi (2000) and Okuyama and Abe (2000). The numerical domains used are usually extended from the experimental one to ensure the flow is fully developed before it reaches the porous sample in a similar manner to that in a wind/water tunnel, in which the flow is smoothed through an extended section before the test section. This addition of an extended domain also helps minimize any numerical instability. In the following simulations, a variable spacing is used in both X and Y directions (longitudinal plane). Meshes close to the walls and in the porous section are finer than the rest of domain. The smallest mesh along the X and Y directions is on the order of 10^{-5} m.

Two-dimensional channel: The physical dimension is 20×10 cm. The porous sample has a length of 2 cm and is situated in the middle of the channel, located between x = 0.09 and 0.11 m. Its geometric structure of pores, the distribution, location and scale are shown in Fig. 1. The porosity is 0.83. The computed results are sampled and presented at 5 locations along the X direction as shown in Fig. 1. The notation, Δ_1-Δ_5, correspond to locations at x = 0.05, 0.09, 0.1, 0.11 and 0.15 m, respectively (porous region lies between Δ_2 and Δ_4). Several different porous structures are analyzed. The aim is to study how the structure of porous medium plays a role in the mass transport and momentum transport, especially the pressure drop. Numerical studies are performed in a range of Reynolds number, $R_{ed} \sim 0.5$-320. A typical inflow velocity is in the range of 0.1-1.0 m sec^{-1}. At the inlet, the fluid enters with a specified mass flow rate and temperature, m and T_{in}, respectively.

Pressure drop and porosity: Non dimensional pressure drop of various porous systems are shown in Table 2. The effects of solid shape and permeability on the sphere-like and fibrous structures are shown in Table 3.

Table 2: Summary of some works in evaluating viscous resistance (pressure drop) in porous media

Assumption	References	Formulation and method	Major results
Periodic porous media, low Reynolds number flow	Larson and Higdon (1992)	Solving stokes flow with a periodic grain consolidation model, collocation method used	Excellent accuracy, moderate computational effort
Incompressible, low Reynolds number flow	Verger and Ladd (1999)	Solving stokes flow, Lattice-Boltzmann method used	Study of the convergence of the permeability as a function of grid resolution for random arrays of spheres-a second order approach
Periodic porous media, low Reynolds number flow	Chapman and Higdon (1992)	Solving unsteady stokes equations, oscillatory pressure gradient imposed	A study in the dynamic permeability and acoustic propagation in porous medium
Incompressible, low Reynolds number flow	Martys and Hagedorn (2002)	Solving Brinkman equation for stokes flow, Lattice-Boltzmann method used	Evaluating permeability in multiple pore size material-low porosity, using parallel computing technique
Incompressible, low Reynolds	Sangani and Yao (1988)	Stokes flow equation	Longitudinal permeability a

Table 3: Non-dimensional pressure drop (P*) of various porous systems against the modified Reynolds number

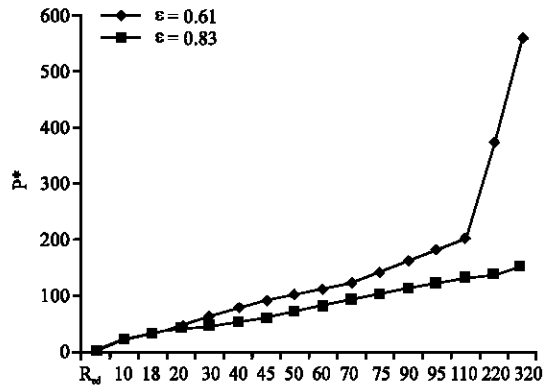| Reynold No.	$\varepsilon = 0.85$	$\varepsilon = 0.89$	$\varepsilon = 0.94$	$\varepsilon = 0.85$
R_{ed}	P*	P*	P*	P*
14	14.50	12.60	7.80	17.60
20	15.00	15.00	7.80	22.00
27	19.50	17.60	8.80	27.00
34	22.00	20.00	10.00	31.00
42	24.00	22.60	10.80	36.00
48	26.00	25.00	12.00	40.00
55	28.00	27.60	13.00	45.00

Fig. 2: Non-dimensional pressure drop P* vs. R_{ed} in a wide range of Reynolds numbers for 2 values of porosities

Fig. 3: A close-up view of the non-dimensional pressure drop P* vs. R_{ed}, exhibiting different behaviors caused by varying porosity ε

The non-dimensional pressure gradient parameter is defined by $P^* = (\Delta p/L)\ l^2/\mu u_{in}$. Here, $\Delta p/L$ is the overall pressure gradient and d is the characteristic solid size. Here, $\Delta p/L$ ($\Delta p = p\ (\Delta_4) - p\ (\Delta_2)$) is the coefficient of viscosity and u_{in} is the approach velocity. Note, the non-dimensional pressure gradient parameter is equivalent to the dimensionless permeability, κ/l^2. The variable P* is used instead in the following discussion. In Table 3, it is evident that the sphere-like structure causes higher pressure drop than the fibrous structure.

The Pressure drops (P*) with respect to the flow conditions (R_{ed}) are shown in Fig. 2 and 3 for two values of porosity. Figure 2 shows the behaviour over a large range of Reynolds numbers in which the behaviour in low
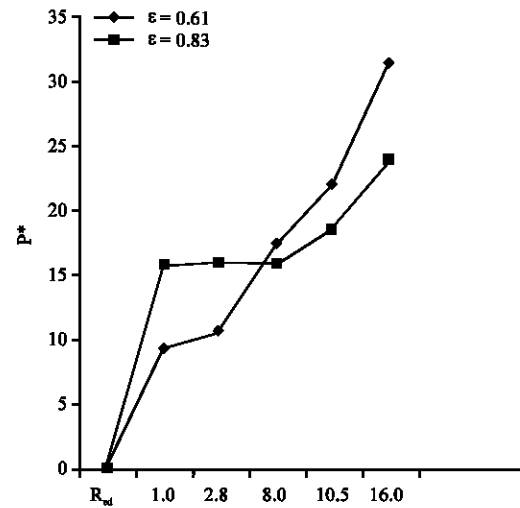
Reynolds number range is shown in a close-up view in Fig. 3. One shows P* approaches a value near 10 as Reynolds tends to zero and there is a larger range where P varies linearly with Reynolds number; this means that the pressure gradient varies as the square of the approach velocity. Thus, the Darcy limit and Forchheimer flow are observed. Moreover, the morphological effect is insignificant if flow is in the low Reynolds number range.

CONCLUSION

The pressure drop is an accumulated result of all factors described in this study and it has been quantitatively predicted at various porosity and topography of different porous media.

REFERENCES

Bear, J., 1972. Dynamics of fluids in porous media. Dover Publications, New York, USA.

Beavers, G.S. and E.M. Sparrow, 1969. Non-Darcy Flow through fibrous porous media. ASME J. Applied Mechanics, 36 (4): 711-714.

Brinkman, H.C., 1947. A calculation of the viscous force extended by a flowing fluid on a dense swarm particles. J. Applied Sci., A 1: 600-616.

Calmidi, V.V., 2000. Forced convection in high porosity metal foams. ASME J. Heat Trans., 122: 557-565.

Chapman, A.M. and J.J. Higdon, 1992. Oscillatory stokes flow in periodic porous media. J. Physical Fluids, A 4: 2099-2116.

Hunt, M.L. and C.L. Tien, 1998a. Effects of thermal dispersion on forced convection in fibrous media. Int. J. Heat Mass Trans., 31 (2): 301-309.

Hunt, M.L. and C.L. Tien, 1998b. Non-Darcian convection in cylindrical packed beds. ASME J. Heat Trans., 110: 378-384.

Kaviany, M., 1991. Principles of heat transfer in porous media. Springer-Verlag Publication, New York.

Large, J.L., B.V. Antohe and D.A. Nield, 1997. Two types of nonlinear pressure-drop versus flow-rate relation observed for saturated porous media. J. Fluids Eng., 119: 700-706.

Larson, R.E. and J.J.L. Higdon, 1992. A periodic grain consolidation of porous media. J. Physical Fluids, A 1: 38-51.

Martys, N.S. and J.G. Hagedorn, 2002. Multiscale modeling of fluid transport in the heterogeneous materials using discrete boltzmann methods. J. Mater. Struct., 35: 650-659.

Okuyama, M. and Y. Abe, 2000. Measurement of velocity and temperature distributions in a highly porous medium. J. Porous Media, 3 (3): 193-206.

Reynolds, O., 1900. Papers on mechanical and physical subjects. Cambridge University Press, Cambridge.

Sahraoui, M. and M. Kaviany, 1993. Slip and no-slip velocity boundary conditions at interface of porous, plain media: Conduction. Int. J. Heat Mass Trans., 36: 1019-1033.

Sangani, A.S. and C. Yao, 1988. Transport processes in random arrays of cylinders II. Viscous flow. J. Physical Fluids, 31: 2435-2444.

Verger, R. and A.J. Ladd, 1999. Simulation of low-reynolds-number flow via a time-independent Lattice-Blotzmann method. Physical Rev. Exercise, 6 (3-8).